NEO: Non Equilibrium Sampling on the Orbit of a Deterministic Transform

Anonymous Author(s)
Affiliation
Address
email

Abstract

Sampling from a complex distribution π and approximating its intractable normalizing constant Z are challenging problems. In this paper, a novel family of importance samplers (IS) and Markov chain Monte Carlo (MCMC) samplers is derived. Given an invertible map T, these schemes combine (with weights) elements from the forward and backward Orbits through points sampled from a proposal distribution ρ. The map T does not leave the target π invariant, hence the name NEO, standing for Non-Equilibrium Orbits. NEO-IS provides unbiased estimators of the normalizing constant and self-normalized IS estimators of expectations under π while NEO-MCMC combines multiple NEO-IS estimates of the normalizing constant and an iterated sampling-importance resampling mechanism to sample from π. For T chosen as a discrete-time integrator of a conformal Hamiltonian system, NEO-IS achieves state-of-the art performance on difficult benchmarks and NEO-MCMC is able to explore highly multimodal targets. Additionally, we provide detailed theoretical results for both methods. In particular, we show that NEO-MCMC is uniformly geometrically ergodic and establish explicit mixing time estimates under mild conditions.

1 Introduction

Consider a target distribution of the form $\pi(x) \propto \rho(x)\mathrm{L}(x)$ where ρ is a probability density function (pdf) on $\mathbb{R}^d$ and L is a nonnegative function. Typically, in a Bayesian setting, π is a posterior distribution associated with a prior distribution ρ and a likelihood function L. An other situation of interest is generative modeling where π is the distribution implicitly defined by a Generative Adversarial Networks (GAN) discriminator-generator pair where ρ is the distribution of the generator and L is derived from the discriminator [31, 6]. An other situation of interest is generative modeling where π is the distribution implicitly defined by a Variational Auto Encoder (VAE) encoder-decoder pair where ρ is the distribution output by the encoder and L is an importance weight between the distribution of the decoder and of the encoder [14, 5]. We are interested in this paper in sampling from π and approximating its intractable normalizing constant $\mathrm{Z} = \int \rho(x)\mathrm{L}(x)\mathrm{d}x$. These problems arise in many applications in statistics, molecular dynamics or machine learning, and remain challenging.

Many approaches to compute normalizing constants are based on Importance Sampling (IS) - see [1, 2] and the references therein - and its variations, among others, Annealed Importance Sampling (AIS) [19, 33, 10] and Sequential Monte Carlo (SMC) [9]. More recently, Neural IS has also become very popular in machine learning; see e.g. [11, 18, 21, 22, 32]. Neural IS is an adaptive IS which relies on an importance function obtained by applying a normalizing flow to a reference distribution. The parameters of this normalizing flow are chosen by minimizing a divergence between the proposal and the target (such as the Kullback-Leibler [18] or the χ^2-divergence [1]).

Submitted to 35th Conference on Neural Information Processing Systems (NeurIPS 2021). Do not distribute.

More recently, the *Non-Equilibrium IS* (NEIS) method has been introduced by [23] as an alternative to these approaches. Similar to Neural IS, NEIS consists in transporting samples $\{X^i\}_{i=1}^N$ from a reference distribution using a family of deterministic mappings. This family for NEIS is chosen to be an homogeneous differential flow $(\phi_t)_{t\in\mathbb{R}}$. In contrast to Neural IS, for any $i \in [N]$, the sample X^i is propagated both forward and backward in time along the orbits associated with $(\phi_t)_{t\in\mathbb{R}}$ until stopping conditions are met. Moreover, the resulting estimator of the normalizing constant is obtained by computing weighted averages of the whole orbit $(\phi_t(X^i))_{t\in[\tau_{+,i},\tau_{-,i}]}$, where $\tau_{+,i}, \tau_{-,i}$ are the resulting stopping times, and not only the endpoints $\phi_{\tau_{+,i}}(X^i), \phi_{\tau_{-,i}}(X^i)$. In [23], the authors provide an application of NEIS with $(\phi_t)_{t\in\mathbb{R}}$ associated with a conformal Hamiltonian dynamics, and reports impressive numerical results on difficult normalizing constants estimation problems, in particular for high-dimensional multimodal distributions.

We propose in this work NEO-IS which alleviates the shortcomings of NEIS. Similar to NEIS, samples are drawn from a reference distribution, typically set to ρ, and are propagated under the forward and backward orbits of a *discrete-time* dynamical system associated with an invertible transform T. An estimator of the normalizing constant is obtained by reweighting all the points on the whole orbits using the IS rule. Contrary to NEIS, the NEO-IS estimator of Z is unbiased under assumptions that are mild and easy to verify. It is more flexible than NEIS because it does not rely on the accuracy of the discretization of a continuous-time dynamical system.

We then show how it is possible to leverage the unbiased estimator of Z defined by NEO-IS to obtain NEO-MCMC, a novel massively parallel MCMC algorithm to sample from π. In a nutshell, NEO-MCMC relies on parallel walkers which each estimates the normalizing constant but are allowed to interact through a resampling mechanism.

Our contributions can be summarized as follows.

- **(i)** We present a novel class of IS estimators of the normalizing constant Z referred to as NEO-IS. More broadly, a small modification of this algorithm also allows us to estimate integrals with respect to π. Both finite sample and asymptotic guarantees are provided for these two methodologies.
- **(ii)** We develop a new massively parallel MCMC method, NEO-MCMC. NEO-MCMC combines NEO-IS unbiased estimator of the normalizing constant with iterated sampling-importance resampling methods. We prove that it is π-reversible and ergodic under very general conditions. We derive also conditions which imply that NEO-MCMC is uniformly geometrically ergodic (with an explicit expression of the mixing time).
- **(iii)** We illustrate our findings using numerical benchmarks which show that both NEO-IS and NEO-MCMC outperform state-of-the-art (SOTA) methods in difficult settings.

2 NEO-IS algorithm

In this section, we derive the NEO-IS algorithm. The two key ingredients for this algorithm are (1) the reference distribution ρ and (2) a transformation T assumed to be a C^1-diffeomorphism with inverse T^{-1}. Write, for $k \in \mathbb{N}^* = \mathbb{N} \setminus \{0\}$, $\mathrm{T}^k = \mathrm{T} \circ \mathrm{T}^{k-1}$, $\mathrm{T}^0 = \mathrm{Id}_d$ and similarly $\mathrm{T}^{-k} = \mathrm{T}^{-1} \circ \mathrm{T}^{-(k-1)}$. For any $k \in \mathbb{Z}$, denote by $\rho_k : \mathbb{R}^d \to \mathbb{R}_+$ the pushforward of ρ by T^k, defined for $x \in \mathbb{R}^d$ by $\rho_k(x) = \rho(\mathrm{T}^{-k}(x))\mathbf{J}_{\mathrm{T}^{-k}}(x)$, where $\mathbf{J}_\Phi(x) \in \mathbb{R}^+$ is the absolute value of the Jacobian determinant of $\Phi : \mathbb{R}^d \to \mathbb{R}^d$ evaluated at x. In line with multiple importance sampling *à la* Owen and Zhou [20], we introduce the proposal density

$$\rho_{\mathrm{T}}(x) = \Omega^{-1} \sum\nolimits_{k\in\mathbb{Z}} \varpi_k \rho_k(x) \ , \tag{1}$$

where $\{\varpi_k\}_{k\in\mathbb{Z}}$ is a nonnegative sequence and $\Omega = \sum_{k\in\mathbb{Z}} \varpi_k$. Note that we assume in the sequel that the support of the weight sequence defined as $\{k \in \mathbb{Z} : \varpi_k \neq 0\}$ is finite. Thus, the mixture distribution in (1) is a **finite mixture**. Given $x \in \mathbb{R}^d$, $\rho_{\mathrm{T}}(x)$ is a function of the forward and backward orbit of T through x.

For any nonnegative function f, the definition of ρ_{T} implies that $\int f(y)\rho_{\mathrm{T}}(y)\mathrm{d}y = \Omega^{-1} \int \sum_{k\in\mathbb{Z}} \varpi_k f(\mathrm{T}^k(x))\rho(x)\mathrm{d}x$. Assuming that $\varpi_0 > 0$, the ratio $\rho(x)/\rho_{\mathrm{T}}(x) \leq \varpi_0^{-1}\Omega < \infty$ is

bounded. We can therefore apply the IS principle which allows to write the identity

$$\boxed{\int f(x)\rho(x)\mathrm{d}x = \int \left(f(y)\frac{\rho(y)}{\rho_{\mathrm{T}}(y)} \right) \rho_{\mathrm{T}}(y)\mathrm{d}y = \int \sum_{k\in\mathbb{Z}} f(\mathrm{T}^k(x))w_k(x)\rho(x)\mathrm{d}x \ ,} \tag{2}$$

where the weights are given by (see Appendix A.1 for a detailed derivation),

$$w_k(x) = \varpi_k \rho(\mathrm{T}^k(x))/\{\Omega\rho_{\mathrm{T}}(\mathrm{T}^k(x))\} = \varpi_k\rho_{-k}(x) \Big/ \sum\nolimits_{i\in\mathbb{Z}} \varpi_{k+i}\rho_i(x) \quad . \tag{3}$$

We assume in the sequel that $\varpi_0 > 0$. In particular, note that under this condition, the weights w_k are also upper bounded uniformly in x: for any $x \in \mathbb{R}^d$, $w_k(x) \leq \varpi_k/\varpi_0$. Eqs. (2) and (3) suggest to estimate the integral $\int f(x)\rho(x)\mathrm{d}x$ by $I^{\mathrm{NEO}}_{\varpi,N}(f) = N^{-1}\sum_{i=1}^N \sum_{k\in\mathbb{Z}} w_k(X^i) f(\mathrm{T}^k(X^i))$ where $\{X^i\}_{i=1}^N$ are i.i.d. samples from the proposal ρ, which is denoted by $X^{1:N} \overset{\mathrm{iid}}{\sim} \rho$.

This estimator is obtained by a weighted combination of the elements of the independent forward and backward orbits $\{\mathrm{T}^k(X^i)\}_{k\in\mathbb{Z}}$ with $X^{1:N} \overset{\mathrm{iid}}{\sim} \rho$. This estimator is referred to as NEO-IS. Choosing $f \equiv \mathrm{L}$ provides the NEO-IS estimator of the normalizing constant of π:

Algorithm 1 NEO-IS Sampler

1. Sample $X^{1:N} \overset{\mathrm{iid}}{\sim} \rho$ for $i \in [N]$.
2. For $i \in [N]$, compute the path $(\mathrm{T}^j(X^i))_{j=0}^K$ and weights $(w_j(X^i))_{j\in\mathbb{Z}}$.
3. $I^{\mathrm{NEO}}_{\varpi,N}(f) = N^{-1}\sum_{i=1}^N \sum_{k=0}^K w_k(X^i) f(\mathrm{T}^k(X^i))$.

$$\widehat{\mathrm{Z}}^{\varpi}_{X^i} = \sum\nolimits_{k\in\mathbb{Z}} \mathrm{L}(\mathrm{T}^k(X^i))w_k(X^i) \ , \quad \widehat{\mathrm{Z}}^{\varpi}_{X^{1:N}} = N^{-1}\sum\nolimits_{i=1}^N \widehat{\mathrm{Z}}^{\varpi}_{X^i} \ . \tag{4}$$

We now study the performance of the NEO-IS estimator. The following two quantities play a fundamental role in the analysis:

$$E^{\varpi}_{\mathrm{T}} = \mathbb{E}_{X\sim\rho}\big[\big(\sum\nolimits_{k\in\mathbb{Z}} w_k(X)\mathrm{L}(\mathrm{T}^k(X))/\,\mathrm{Z}\big)^2\big], M^{\varpi}_{\mathrm{T}} = \sup\nolimits_{x\in\mathbb{R}^d} \sum\nolimits_{k\in\mathbb{Z}} w_k(x)\mathrm{L}(\mathrm{T}^k(x))/\,\mathrm{Z} \ . \tag{5}$$

Theorem 1. *$\widehat{\mathrm{Z}}^{\varpi}_{X^{1:N}}$ is an unbiased estimator of Z. If $E^{\varpi}_{\mathrm{T}} < \infty$, then, $\mathbb{E}[|\widehat{\mathrm{Z}}^{\varpi}_{X^{1:N}}/\,\mathrm{Z} - 1|^2] = N^{-1}(E^{\varpi}_{\mathrm{T}} - 1)$. If $M^{\varpi}_{\mathrm{T}} < \infty$, then, for any $\delta \in (0,1)$, with probability $1-\delta$, $\sqrt{N}\left|\widehat{\mathrm{Z}}^{\varpi}_{X^{1:N}}/\,\mathrm{Z} - 1\right| \leq M^{\varpi}_{\mathrm{T}}\sqrt{\log(2/\delta)/2}$.*

The (elementary) proof is postponed to Appendix A.2. E^{ϖ}_{T} plays the role of the second-order moment of the importance weights $\mathbb{E}_{X\sim\rho}[\mathrm{L}^2(X)]$ which is key to the performance of IS algorithms [1, 2]. In addition, since the NEO-IS estimator $\widehat{\mathrm{Z}}^{\varpi}_{X^{1:N}}$ is unbiased, the Cauchy-Schwarz inequality shows that $\mathbb{E}_{X\sim\rho}\big[\big(\sum_{k\in\mathbb{Z}} w_k(X)\mathrm{L}(\mathrm{T}^k(X))\big)^2\big] \geq \mathrm{Z}^2$ and hence that $E^{\varpi}_{\mathrm{T}} \geq 1$. Note that if $\|\mathrm{L}\|_\infty = \sup_{x\in\mathbb{R}^d}\mathrm{L}(x) < \infty$, then since the weights are uniformly bounded by $\Omega\varpi_0^{-1}$, we have $M^{\varpi}_{\mathrm{T}} \leq \|\mathrm{L}\|_\infty \Omega\varpi_0^{-1}/\,\mathrm{Z}$.

Using the NEO-IS estimate $\widehat{\mathrm{Z}}^{\varpi}_{X^{1:N}}$ of the normalizing constant, we can construct a self-normalized IS estimate of $\int f(x)\pi(x)\mathrm{d}x$:

$$J^{\mathrm{NEO}}_{\varpi,N}(f) = N^{-1}\sum_{i=1}^N \frac{\widehat{\mathrm{Z}}^{\varpi}_{X^i}}{\widehat{\mathrm{Z}}^{\varpi}_{X^{1:N}}} \sum_{k\in\mathbb{Z}} \frac{\mathrm{L}(\mathrm{T}^k(X^i))w_k(X^i)}{\widehat{\mathrm{Z}}^{\varpi}_{X^i}} f(\mathrm{T}^k(X^i)) \ , \tag{6}$$

referred to as NEO-SNIS estimator. This expression may seem unnecessarily complicated but highlights the hierarchical structure of the estimator. We combine estimators $(\widehat{\mathrm{Z}}^{\varpi}_{X^i})^{-1}\sum_{k\in\mathbb{Z}} \mathrm{L}(\mathrm{T}^k(X^i))w_k(X^i)f(\mathrm{T}^k(X^i))$ evaluated on the forward and backward orbits through the points $\{X^i\}_{i=1}^N$ using weights $\{\widehat{\mathrm{Z}}^{\varpi}_{X^i}/\widehat{\mathrm{Z}}^{\varpi}_{X^{1:N}}\}_{i=1}^N$. Although the NEO-IS estimator is unbiased, the NEO-SNIS is in general biased. However, for bounded functions, both the bias and the variance of the NEO-SNIS estimator are $O(N^{-1})$, with constants proportional to E^{ϖ}_{T}. For g a bounded function, define $\pi(g) = \int g(x)\pi(x)\mathrm{d}x$.

Theorem 2. *Assume that $E^{\varpi}_{\mathrm{T}} < \infty$. Then, for any function g satisfying $\sup_{x\in\mathbb{R}^d}|g(x)| \leq 1$ on $\mathbb{R}^d$, and $N \in \mathbb{N}$*

$$\mathbb{E}_{X^{1:N}\overset{\mathrm{iid}}{\sim}\rho}\left[|J^{\mathrm{NEO}}_{\varpi,N}(g) - \pi(g)|^2\right] \leq 4\cdot N^{-1}E^{\varpi}_{\mathrm{T}} \ , \tag{7}$$

$$\left|\mathbb{E}_{X^{1:N}\overset{\mathrm{iid}}{\sim}\rho}\left[J^{\mathrm{NEO}}_{\varpi,N}(g) - \pi(g)\right]\right| \leq 2\cdot N^{-1}E^{\varpi}_{\mathrm{T}} \ . \tag{8}$$

If $M_{\mathrm{T}}^{\varpi} < \infty$, then for $\delta \in (0,1]$, with probability at least $1-\delta$,

$$\sqrt{N}|J_{\varpi,N}^{\mathrm{NEO}}(g) - \pi(g)| \leq \|g\|_{\infty} M_{\mathrm{T}}^{\varpi} \sqrt{32\log(4/\delta)} \ . \tag{9}$$

The proof is postponed to Appendix A.3. These results extend to NEO-SNIS estimators the results known for self-normalized estimators; see e.g., [1, 2] and the references therein. The upper bounds stated in this result suggest it is good practice to keep $E_{\mathrm{T}}^{\varpi}/N$ small in order to obtain sensible approximations. For two pdfs p and q on $\mathbb{R}^d$, denote by $\mathrm{D}_{\chi^2}(p,q) = \int \{p(x)/q(x) - 1\}^2 q(x)\mathrm{d}x$ the χ^2-divergence between p and q.

Lemma 3. *For any nonnegative sequence $(\varpi_k)_{k\in\mathbb{Z}}$, we have $E_{\mathrm{T}}^{\varpi} \leq \mathrm{D}_{\chi^2}(\pi\|\rho_{\mathrm{T}}) + 1$.*

The proof is postponed to Appendix A.4. Lemma 3 suggests that accurate sampling requires N to scale linearly with the χ^2-divergence between the target π and the extended proposal ρ_{T}.

Remark 1. We can extend NEO to non homogeneous flows, replacing the family $\{\mathrm{T}^k : k \in \mathbb{Z}\}$ with a collection of mappings $\{\mathsf{T}_k : k \in \mathbb{Z}\}$. This would allow us to consider further flexible classes of transformations such as normalizing flows; see e.g. [21]. The χ^2-divergence $\mathrm{D}_{\chi^2}(\pi\|\rho_{\mathrm{T}})$ provides natural criteria for learning the transformation. We leave this extension to future work.

Conformal Hamiltonian transform The efficiency of NEO relies heavily on the choice of T. Intuitively, a sensible choice of T requires that (i) E_{T}^{ϖ} is small, i.e. ρ_{T} should be close to π by Lemma 3 (see (5)), (ii) the inverse T^{-1} and the Jacobian of T are easy to compute. Following [23], we use for T a discretization of a conformal Hamiltonian dynamics. Assume that $U(\cdot) = -\log\pi(\cdot)$ is continuously differentiable. We consider the augmented distribution $\tilde{\pi}(q,p) \propto \exp\{-U(q) - K(p)\}$ on $\mathbb{R}^{2d}$, where q is the position, p is the momentum, and $K(p) = p^T\mathrm{M}^{-1}p/2$ is the kinetic energy, with M a positive definite mass matrix. By construction, the marginal distribution of the momentum under $\tilde{\pi}$ is the target pdf $\pi(q) = \int \tilde{\pi}(q,p)\mathrm{d}p$. The conformal Hamiltonian ODE associated with $\tilde{\pi}$ is defined by

$$\begin{aligned} \mathrm{d}q_t/\mathrm{d}t &= \nabla_p H(q_t,p_t) = \mathrm{M}^{-1}p_t \ , \\ \mathrm{d}p_t/\mathrm{d}t &= -\nabla_q H(q_t,p_t) - \gamma p_t = -\nabla U(q_t) - \gamma p_t \ , \end{aligned} \tag{10}$$

where $H(q,p) = U(q) + K(p)$, and $\gamma > 0$ is a damping constant. Any solution $(q_t,p_t)_{t\geq 0}$ of (10) satisfies setting $H_t = H(q_t,p_t)$, $\mathrm{d}H_t/\mathrm{d}t = -\gamma p_t^T\mathrm{M}^{-1}p_t \leq 0$. Hence, all orbits converge to fixed points that satisfy $\nabla U(q) = 0$ and $p = 0$; see e.g. [12, 17].

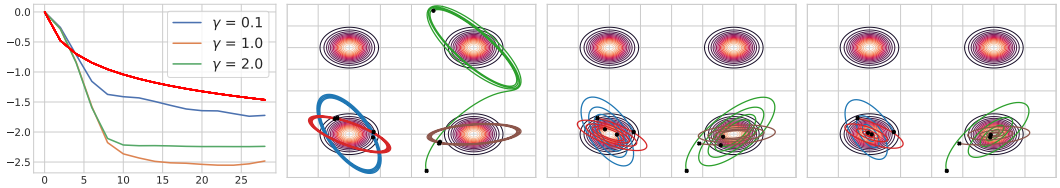

Figure 1: Left: $E_{\mathrm{T}_h}^{\mathbb{1}_{[K]}}(K)$ vs $E^{\mathrm{IS}}(K)$ (red) in $\log_{10}$-scale as a function of optimization step K. Second left to right: Corresponding orbits for $\gamma = 0.1, 1, 2$.

In the applications below, we consider the conformal version of the symplectic Euler (SE) method of (10), see [12]. This integrator can be constructed as a splitting of the two conformal and conservative parts of the system (10). When composing a dissipative with a symplectic operator, we set for all $(q,p) \in \mathbb{R}^{2d}$, $\mathrm{T}_h(q,p) = (q + h\mathrm{M}^{-1}\{\mathrm{e}^{-h\gamma}p - h\nabla U(q)\}, \mathrm{e}^{-h\gamma}p - h\nabla U(q))$, where $h > 0$ is a discretization stepsize. This transformation can be connected with classical momentum optimization schemes, see [12, Section 4]. By [12, Section 3], for any $h > 0$ T_h is a C^1-diffeomorphism on $\mathbb{R}^{2d}$ with Jacobian given by $\mathbf{J}_{\mathrm{T}_h}(q,p) = \mathrm{e}^{-\gamma hd}$. In addition, its inverse is $\mathrm{T}_h^{-1}(q,p) = (q - h\mathrm{M}^{-1}p, \mathrm{e}^{\gamma h}\{p + h\nabla U(q - h\mathrm{M}^{-1}p)\})$. Therefore, the weight (3) of the NEO estimator is given by

$$w_k(q,p) = \frac{\varpi_k \tilde{\rho}(\mathrm{T}_h^k(q,p))\mathrm{e}^{-\gamma khd}}{\sum_{j\in\mathbb{Z}} \varpi_{k+j}\tilde{\rho}(\mathrm{T}_h^j(q,p))\mathrm{e}^{-\gamma jhd}} \ ,$$

where $\tilde{\rho}(q,p) \propto \rho(q)\mathrm{e}^{-K(p)}$. Figure 1 displays for different values of γ, the bound $E_{\mathrm{T}_h}^{\mathbb{1}_{[0:K]}} - 1$ (5) as a function of K corresponding to the sequence of weights $(\varpi_k)_{k\in\mathbb{Z}} = (\mathbb{1}_{[0:K]}(k))_{k\in\mathbb{Z}}$ (i.e. only

the $K+1$ first elements of the forward orbits are used and are equally weighted). For comparison, we also present on the same plot, the bounds achieved by averaging $K+1$ independent IS estimates, $E^{\mathrm{IS}}(K) - 1 = (K+1)^{-1}\mathbb{E}_{X\sim\rho}[\mathrm{L}(X))^2]$. Interestingly, Figure 1 shows that there is a trade-off in the choice of γ which controls the exploration of the state space by the Hamiltonian dynamics since the higher γ, the faster the orbits converge towards the modes.

3 NEO-MCMC algorithm

We now derive sampling methods based on the NEO-IS estimator. A natural idea consists in adapting the Sampling Importance Resampling procedure (SIR) (see for example [24, 27]) to the NEO framework.

The SIR method to sample $J^{\mathrm{NEO}}_{\varpi,N}$ (see (6)) consists of 4 steps.

(SIR-1) Draw independently $X^{1:N} \overset{\mathrm{iid}}{\sim} \rho$ and compute the associated forward and backward orbits $\{\mathrm{T}^k(X^i)\}_{k\in\mathbb{Z}}$ of the point.

(SIR-2) Compute the normalizing constants associated with each orbit $\{\widehat{\mathrm{Z}}^{\varpi}_{X^i}\}_{i=1}^N$.

(SIR-3) Sample an orbit index $I_N \in [N]$ with probability $\{\widehat{\mathrm{Z}}^{\varpi}_{X^i}/\sum_{j=1}^N \widehat{\mathrm{Z}}^{\varpi}_{X^j}\}_{i=1}^N$.

(SIR-4) Draw the iteration index K^N on the I^N-th orbit with probability $\{\mathrm{L}(\mathrm{T}^k(X^{I^N}))w_k(X^{I^N})/\widehat{\mathrm{Z}}^{\varpi}_{X^{I^N}}\}_{k\in\mathbb{Z}}$.

The resulting draw is denoted by $U^N = \mathrm{T}^{K^N}(X^{I^N})$. By construction, for any bounded function f, we get that $\mathbb{E}\left[f(U^N)\middle|X^{1:N}, I^N\right] = \{\widehat{\mathrm{Z}}^{\varpi}_{X^{I^N}}\}^{-1}\sum_{k\in\mathbb{Z}} w_k(X_{I^N})\mathrm{L}(\mathrm{T}^k(X_{I^N}))$ which implies $\mathbb{E}\left[f(U^N)\middle|X^{1:N}, I^N\right] = J^{\mathrm{NEO}}_{\varpi,N}(f)$ (see (6)). Using Theorem 2, we therefore obtain $|\mathbb{E}[f(U^N)] - \int f(z)\pi(z)\mathrm{d}z| \leq 10^{1/2}\|f\|_\infty E^{\varpi}_{\mathrm{T}} N^{-1}$, showing that the law of the random variable $\mu_N = \mathrm{Law}(U^N)$ converges in total variation to π as $N \to \infty$,

$$\|\mu_N - \pi\|_{\mathrm{TV}} = \sup_{\|f\|_\infty \leq 1} |\mu_N(f) - \pi(f)| \leq 10^{1/2} E^{\varpi}_{\mathrm{T}} N^{-1} . \tag{11}$$

Algorithm 2 NEO-MCMC Sampler

At step $n \in \mathbb{N}^*$, given the conditioning orbit point Y_{n-1}.

Step 1: Update the conditioning point

1. Set $X^1_n = Y_{n-1}$ and for any $i \in \{2,\ldots,N\}$, sample $X^i_n \overset{\mathrm{iid}}{\sim} \rho$.
2. Sample the orbit index I_n with probability proportional to $(\widehat{\mathrm{Z}}^{\varpi}_{X^i_n})_{i\in[N]}$, (4).
3. Set $Y_n = X^{I_n}_n$

Step 2: Output a sample

4. Sample index K_n with probability proportional to $\{w_k(Y_n)\mathrm{L}(\mathrm{T}^k(Y_n))/\widehat{\mathrm{Z}}^{\varpi}_{Y_n}\}_{k\in\mathbb{Z}}$
5. Output $U_n = \mathrm{T}^{K_n}(Y_n)$.

Based on [3], we now derive the NEO-MCMC procedure, which in a nutshell consists in iterating the SIR procedure while keeping a conditioning point (or equivalently, orbit); see Appendix C. The convergence of NEO-MCMC does not rely on letting $N \to \infty$: the NEO-MCMC works as soon as $N \geq 2$, although as we will see below the mixing time decreases as N increases.

This procedure is summarized in Algorithm 2. The NEO-MCMC procedure is an iterated algorithm which produces a sequence $\{(Y_n, U_n)\}_{n\in\mathbb{N}}$ of points in $\mathbb{R}^d$. The n-th iteration of the NEO-MCMC algorithm consists in two main steps: 1) updating the conditioning point $Y_{n-1} \to Y_n$ 2) sampling U_n by selecting a point in the orbit $\{\mathrm{T}^k(Y_n)\}_{k\in\mathbb{Z}}$ of the conditioning point. Compared to SIR, only the generation of the points (step (SIR-1)) is modified: we set $X^1_n = Y_{n-1}$ (the **conditioning point**), and then draw $X^{2:N}_n \overset{\mathrm{iid}}{\sim} \rho$.

The sequence $\{Y_n\}_{n\in\mathbb{N}}$ defined by Algorithm 2 is a Markov chain: $\mathbb{P}\left(Y_n \in \mathsf{A} \,|\, Y_{0:n-1}\right) = \mathbb{P}\left(Y_n \in \mathsf{A} \,|\, Y_{n-1}\right) = P(Y_n, \mathsf{A})$ where

$$P(y, \mathsf{A}) = \int \delta_y(\mathrm{d}x^1) \prod_{j=2}^N \rho(x^j)\mathrm{d}x^j \sum_{i=1}^N \frac{\widehat{\mathrm{Z}}^{\varpi}_{x^i}}{\sum_{j=1}^N \widehat{\mathrm{Z}}^{\varpi}_{x^j}} \mathbb{1}_{\mathsf{A}}(x^i) , \quad y \in \mathbb{R}^d , \mathsf{A} \in \mathcal{B}(\mathbb{R}^d) . \tag{12}$$

Note that this Markov kernel describes the way, at stage $n+1$, the conditioning point Y_{n+1} is selected given Y_n, which **depends only on** the estimator of the normalizing constants associated with each orbit, **but not** on the sample U_n selected on the conditioning orbit. In addition, given the

conditioning point Y_n at the n-th iteration, the conditional distribution of the output sample U_n is $\mathbb{P}\left(U_n \in \mathsf{B} \,|\, I_n, X_n^{1:N}\right) = \mathbb{P}\left(U_n \in \mathsf{B} \,|\, Y_n\right) = Q(Y_n, \mathsf{B})$ where

$$Q(y, \mathsf{B}) = \sum_{k \in \mathbb{Z}} \frac{w_k(y) \mathrm{L}(\mathrm{T}^k(y))}{\widehat{\mathrm{Z}}_y^{\varpi}} \mathbb{1}_{\mathsf{B}}(\mathrm{T}^k(y)) \ , \quad y \in \mathbb{R}^d \ , \mathsf{B} \in \mathcal{B}(\mathbb{R}^d) \ . \tag{13}$$

With these notations, if the Markov chain is started at $Y_0 = y$, then for any $n \in \mathbb{N}$, the law of the n-th conditioning point is $\mathbb{P}\left(Y_n \in \mathsf{A} \,|\, Y_0 = y\right) = P^n(y, \mathsf{A})$ and the law of the n-th sample is $\mathbb{P}\left(U_n \in \mathsf{B} \,|\, Y_0\right) = P^n Q(y, \mathsf{B})$. Define $\tilde{\pi}$ the pdf given, for $y \in \mathbb{R}^d$, by

$$\tilde{\pi}(y) = \frac{\rho(y)}{\mathrm{Z}} \sum_{k \in \mathbb{Z}} w_k(y) \mathrm{L}(\mathrm{T}^k(y)) = \frac{\rho(y) \widehat{\mathrm{Z}}_y^{\varpi}}{\mathrm{Z}} \ . \tag{14}$$

The following theorem shows that, for any initial condition $y \in \mathbb{R}^d$, the distribution of the variable Y_n converges in total variation to $\tilde{\pi}$ and that the distribution of U_n converges to π.

Theorem 4. *The Markov kernel P is reversible with respect to the distribution $\tilde{\pi}$, ergodic and Harris positive, i.e., for all $y \in \mathbb{R}^d$, $\lim_{n \to \infty} \|P^n(y, \cdot) - \tilde{\pi}\|_{\mathrm{TV}} = 0$. In addition, $\pi = \tilde{\pi} Q$ and $\lim_{n \to \infty} \|P^n Q(y, \cdot) - \pi\|_{\mathrm{TV}} = 0$. Moreover, for any bounded function g and any $y \in \mathbb{R}^d$, $\lim_{n \to \infty} n^{-1} \sum_{i=0}^{n-1} g(U_i) = \pi(g)$, $\mathbb{P}_y$-almost surely.*

The proof is postponed to Appendix A.5.

Remark 2. We may provide another sampling procedure of $\{Y_n\}_{n \in \mathbb{N}}$. Define the pdf on the extended space $[N] \times \mathbb{R}^{dN}$ by $\check{\pi}(i, x^{1:N}) = N^{-1} \tilde{\pi}(x^i) \prod_{j=1, j \neq i}^N \rho(x^j)$. Consider a Gibbs sampler targeting $\check{\pi}$ consisting in (a) sampling $X_n^{1:N \setminus \{I_{n-1}\}} | (I_{n-1}, X_{n-1}) \sim \prod_{j \neq I_{n-1}} \rho(x^j)$, (b) sampling $I_n | X_n^{1:N} \sim \mathrm{Cat}(\{\widehat{\mathrm{Z}}_{X_n^i}^{\varpi} / \sum_{j=1}^N \widehat{\mathrm{Z}}_{X_n^j}^{\varpi}\}_{i=1}^N$ and (c) set $Y_n = X_n^{I_n}$. This algorithm is a Gibbs sampler on $\check{\pi}$ and we easily verify that the distribution of $\{Y_n\}_{n \in \mathbb{N}}$ is the same as Algorithm 2.

The next theorem provides non asymptotic quantitative bounds on the convergence in total variation. The main interest of NEO-MCMC algorithm is motivated empirically from observed behaviour: the mixing time of the corresponding Markov chain improves as N increases. This behaviour is quantified theoretically in the next theorem. Moreover, this improvement is obtained with little extra computational overhead, since sampling N points from the proposal distribution ρ, computing the forward and backward orbits of the points and evaluating the normalizing constants $\{\widehat{\mathrm{Z}}_{X_n^i}^{\varpi}\}_{i=1}^N$ can be performed in parallel.

Theorem 5. *Assume that $M_{\mathrm{T}}^{\varpi} < \infty$, see (5). Set $\epsilon_N = (N-1)/(2M_{\mathrm{T}}^{\varpi} + N - 2)$ and $\kappa_N = 1 - \epsilon_N$. Then, for any $y \in \mathbb{R}^d$ and $k \in \mathbb{N}$, $\|P^k(y, \cdot) - \tilde{\pi}\|_{\mathrm{TV}} \leq \kappa_N^k$ and $\|P^k Q(y, \cdot) - \pi\|_{\mathrm{TV}} \leq \kappa_N^k$.*

Instead of sampling the new points $X_n^{2:N}$ independently from ρ (Step 1 in Algorithm 2), it is possible to draw the proposals $X_n^{1:N}$ conditional to the current point Y_{n-1}; see [29, 8, 26, 25] for related works. Following [25], we use a reversible Markov kernel with respect to the proposal ρ, i.e., such that $\rho(x) m(x, x') = \rho(x') m(x', x)$, assuming for simplicity that this kernel has density $m(x, x')$. If $\rho = \mathrm{N}(0, \sigma^2 \mathrm{Id}_d)$, an appropriate choice is an autoregressive kernel $m(x, x') = \mathrm{N}(x'; \alpha x, \sigma^2 (1 - \alpha^2) \mathrm{Id}_d)$. More generally, we can use a Metropolis–Hastings kernel with invariant distribution ρ. In this case, for each $i \in [N]$, define for $i \in [N]$,

$$r_i(y, x^{1:N \setminus \{i\}}) = \prod_{j=2}^{i-1} m(x^{j-1}, x^j) \prod_{j=i+1}^{N} m(x^{j-1}, x^j) \ . \tag{15}$$

Since m is reversible with respect to ρ, for all $i, j \in [N]$, $\rho(x^i) r_i(x^i, x^{1:N \setminus \{i\}}) = \rho(x^j) r_j(x^j, x^{1:N \setminus \{j\}})$. The only modification in Algorithm 2 is Step 1, which is replaced by: *Draw $U_n \in [N]$ uniformly, set $X_n^{U_n} = Y_{n-1}$ and sample $X_n^{1:N \setminus \{U_n\}} \sim r_{U_n}(X_n^{U_n}, \cdot)$.* The validity of this procedure is established in Appendix A.5.

4 Continuous-time version of NEO and NEIS

The NEO framework takes up and extends NEIS introduced in [23]. NEIS focuses on normalizing constant estimation and should be therefore compared with NEO-IS. In [23], the authors do not

consider possible extensions of these ideas to sampling problems. Proofs of the statements and detailed technical conditions are postponed to Appendix B. We first consider how NEO can be adapted to continuous-time dynamical system. Consider the Ordinary Differential Equation (ODE) $\dot{x}_t = b(x_t)$, where $b\colon \mathbb{R}^d \to \mathbb{R}^d$ is a smooth vector field. Denote by $(\phi_t)_{t\in\mathbb{R}}$ the flow of this ODE (assumed to be well-behaved). Under appropriate regularity condition $\mathbf{J}_{\phi_t}(x) = \exp(\int_0^t \nabla \cdot b(\phi_s(x))\mathrm{d}s)$; see Lemma S4. Let $\varpi : \mathbb{R} \to \mathbb{R}_+$ be a nonnegative smooth function with finite support, with $\Omega^c = \int_{-\infty}^{\infty} \varpi(t)\mathrm{d}t$. The continuous-time counterpart of the proposal distribution (1) is $\rho_{\mathrm{T}}^{\mathrm{c}}(x) = (\Omega^c)^{-1} \int_{-\infty}^{\infty} \varpi(t)\rho(\phi_{-t}(x))\mathbf{J}_{\phi_{-t}}(x)\mathrm{d}t$, which is a continuous mixture of the pushforward of the proposal ρ by the flow of $(\phi_s)_{s\in\mathbb{R}}$. Assuming for simplicity that $\rho(x) > 0$ for all $x \in \mathbb{R}^d$, then $\rho_{\mathrm{T}}^{\mathrm{c}}(x) > 0$ for all $x \in \mathbb{R}^d$, and using again the IS formula, for any nonnegative function f,

$$\int f(x)\rho(x)\mathrm{d}x = \int f(x)\frac{\rho(x)}{\rho_{\mathrm{T}}^{\mathrm{c}}(x)}\rho_{\mathrm{T}}^{\mathrm{c}}(x)\mathrm{d}x = \int \left[\int_{-\infty}^{\infty} w_t^{\mathrm{c}}(x) f(\phi_t(x))\mathrm{d}t\right]\rho(x)\mathrm{d}x \ , \tag{16}$$

$$w_t^{\mathrm{c}}(x) = \varpi(t)\rho(\phi_t(x))\mathbf{J}_{\phi_t}(x) \Big/ \int_{-\infty}^{\infty} \varpi(s+t)\rho(\phi_s(x))\mathbf{J}_{\phi_s}(x)\mathrm{d}s \ . \tag{17}$$

These relations are the continuous-time counterparts of (2). Eqs. (16)-(17) define a version of NEIS [23], with a finite support weight function ϖ; see Appendices B.2 and B.3 for weight functions with infinite support. This identity is of theoretical interest but must be discretized to obtain a computationally tractable estimator. For $h > 0$, denote by T_h an integrator with stepsize $h > 0$ of the ODE $\dot{x} = b(x)$. We may construct NEO-IS and NEO-SNIS estimators based on the transform $\mathrm{T} \leftarrow \mathrm{T}_h$ and weights $\varpi_k \leftarrow \varpi(kh)$. Provided that the order of the integrator is larger than 2, then for any $x \in \mathbb{R}^d$, $\sum_{k\in\mathbb{Z}} w_k(x) f(\mathrm{T}_h^k(x)) = \int_{-\infty}^{\infty} w_t^{\mathrm{c}}(x) f(\phi_t(x))\mathrm{d}t + O(h)$. Therefore, taking $h \downarrow 0^+$, the NEO-IS converges to the continuous-version (16)-(17). There is however an important difference between NEO and the NEIS method in [23] which stems from the way (16)-(17) are discretized. Compared to NEIS, NEO-IS using $\mathrm{T} \leftarrow \mathrm{T}_h$ and weights $\varpi_k \leftarrow \varpi(kh)$ is unbiased for any stepsize $h > 0$. NEIS uses an approach inspired by the nested-sampling approach, which amounts to discretizing the integral in (16) also in the state-variable x; see [28, 7]. This discretization is biased which prevents the use of this approach to develop MCMC sampling algorithm; see Appendix B.

5 Experiments and Applications

Normalizing constant estimation The performance of NEO-IS is assessed on different normalizing constant estimation benchmarks; see [13]. We focus on two challenging examples. Additional experiments and discussion on hyperparameter choice are given in the supplementary material, see Appendix D. **(1) Mixture of Gaussian** `(MG25)`: $\pi(x) = P^{-1}\sum_{i=1}^{P} \mathrm{N}(x; \mu_{i,j}, D_d)$, where $d \in \{10, 20, 40\}$, $D_d = \mathrm{diag}(0.01, 0.01, 0.1, \ldots, 0.1)$ and $\mu_{i,j} = [i, j, 0, \ldots, 0]^T$ with $i, j \in \{-2, \ldots, 2\}$. **(2) Funnel distribution** `(Fun)` $\pi(x) = \mathrm{N}(x_1; 0, a^2)\prod_{i=1}^{d} \mathrm{N}(x_i; 0, \mathrm{e}^{2bx_1})$ with $d \in \{10, 20, 40\}$, $a = 1$, and $b = 0.5$. In both case, the proposal is $\rho = \mathrm{N}(0, \sigma_\rho^2 \mathrm{Id}_d)$ with $\sigma_\rho^2 = 5$.

The NEO-IS estimator is compared with (i) the IS estimator using the proposal ρ, (ii) the Adaptive Importance Sampling (AIS) estimator of [30] and (iii) the Neural Importance Sampling (NIS)[1]. For NEO-IS, we use $\varpi_k = \mathbb{1}_{[K]}(k)$ with $K = 10$ (ten steps on the forward orbit), and conformal Hamiltonian dynamics $\gamma = 1$, $M = 5 \cdot \mathrm{Id}_d$ for dimensions $d = \{10, 20\}$, and $\gamma = 2.5$ for $d = 40$ (where γ is the damping factor, M the mass matrix, h is the stepsize of the integrator). The parameters of AIS are set to obtain a complexity comparable to NEO-IS; see Appendix D. For NIS, we use the default parameters. In `Fun`, we set $\gamma = 0.2$, $K = 10$, $M = 5 \cdot \mathrm{Id}_d$, and $h = 0.3$. The IS estimator was based on $5 \cdot 10^5$ samples, and NIS, NEO-IS and AIS were computed with $5 \cdot 10^4$ samples. Figure 2 shows that NEO-IS consistently outperforms the competing methods.

Sampling NEO-MCMC is assessed for the distributions `(MG25)` ($d = 40$) and `Fun` ($d = 20$). NEO-MCMC sampler is compared with (i) the No-U-Turn Sampler - Pyro library [4] - and (ii) i-SIR algorithm [25]. The proposal distribution is $\rho = \mathrm{N}(0, \sigma_\rho^2 \mathrm{Id}_d)$ with $\sigma_\rho^2 = 5$. Dependent proposals are used (see (15)) with $m(x, x') = \mathrm{N}(x'; \alpha x, \sigma_\rho^2(1-\alpha^2)\mathrm{Id}_d)$ with $\alpha = 0.99$. For NUTS, the default parameters are used. For i-SIR, we use the same number of proposals $N = 10$, proposal distribution

[1] We used the implementation provided by: https://github.com/ndeutschmann/zunis

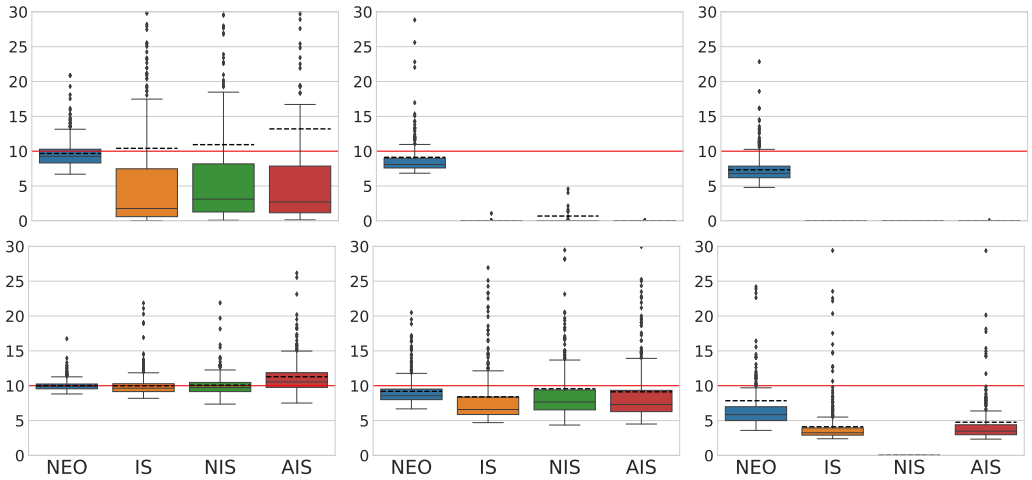

Figure 2: Boxplots of 500 independent estimations of the normalizing constant in dimension $d = \{10, 20, 45\}$ (from left to right) for `MG25` (top) and `Fun` (bottom). The true value is given by the red line. The figure displays the median (solid lines), the interquartile range, and the mean (dashed lines) over the 500 runs.

and dependent proposal as for NEO-MCMC. To make a fair comparison, we use the same clock time for all three algorithms. The number of iterations for correlated i-SIR, NEO-MCMC, and NUTS are $n = 4 \cdot 10^6$, $n = 4 \cdot 10^5$, and $n = 5 \cdot 10^5$, respectively. Figure 3 displays the empirical

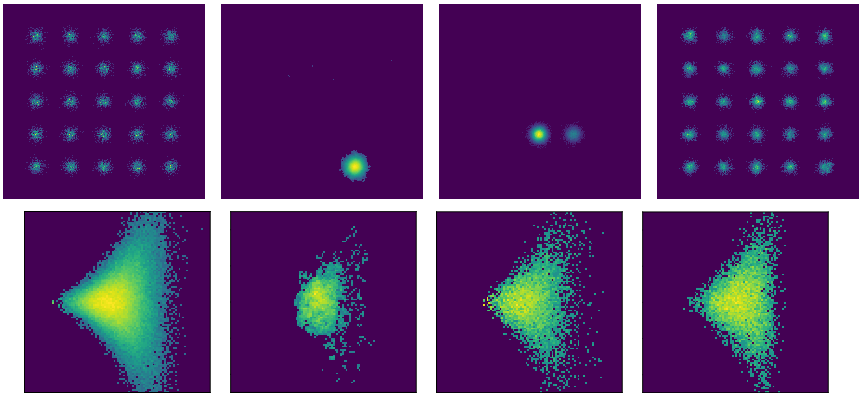

Figure 3: Empirical 2-D histogram of the samples of different algorithms targeting the the *Mixture of Gaussian* example (top) and the *Funnel* example (bottom). From left to right: samples from the target distribution, correlated i-SIR, NUTS, NEO-MCMC.

two-dimensional histograms of the two first coordinates of samples from the ground truth, i-SIR, NUTS and NEO-MCMC sampler. It is worthwhile to note that NEO-MCMC algorithm performs much better for `MG25` which is a very challenging distribution, even for SOTA algorithm such as NUTS, which struggles to cross energy barriers between modes. For `Fun`, NEO-MCMC performs favourably with respect to NUTS, which is well adapted for this type of distributions.

Block Gibbs Inpainting with Deep Generative models and NEO-MCMC We apply NEO-MCMC to the task of sampling the posterior of a deep latent variable model. The model consists of a latent variable $x \sim \mathrm{N}(z; 0, \mathrm{Id}_d)$ and a conditional distribution $p(y \mid x)$ which generates an image $y = (y^1, \ldots, y^D) \in \mathbb{R}^D$. Given a family of parametric *decoders* $\{x \mapsto p_\theta(y \mid x), \theta \in \Theta\}$, and a training set $\mathcal{D} = \{y_i\}_{i=1}^M$, training involves finding the MLE $\theta^* = \arg\max_{\theta \in \Theta} p_\theta(\mathcal{D})$. As $p_\theta(y) = \int p_\theta(y \mid x) p(x) \mathrm{d}x$, the likelihood is intractable and to alleviate this problem, [14] proposed to train jointly an approximate posterior $q_\phi(x|y)$ that maximizes a tractable lower-bound on the log-likelihood: $\mathrm{ELBO}(y, \theta, \phi) = \mathbb{E}_{X \sim q_\phi(\cdot|y)}[\log p_\theta(y, X)/q_\phi(X|y)] \leq p_\theta(y)$, where $q_\phi(x \mid y)$ is a

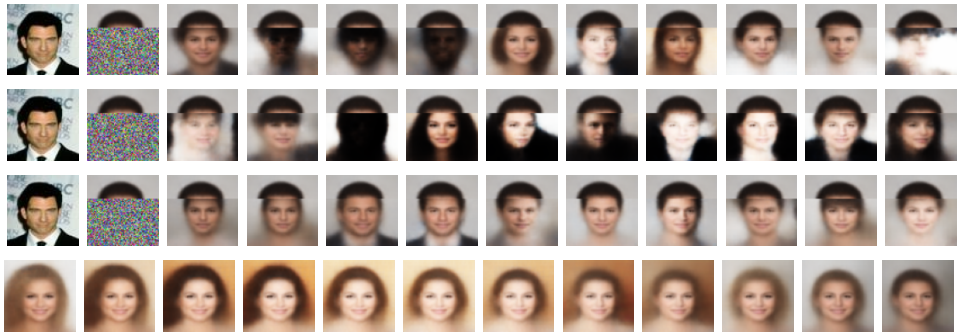

Figure 4: Gibbs inpainting for CelebA dataset. From top to bottom: i-SIR, HMC and NEO-MCMC: From left to right, original image, blurred image to reconstruct, and output every 5 iterations of the Markov chain. Last line: a forward orbit used in NEO-MCMC.

tractable conditional distribution with parameters $\phi \in \Phi$. It is assumed in the sequel that conditional to the latent variable x, the coordinates are independent, *i.e.* $p_\theta(y \mid x) = \prod_{i=1}^{D} p_\theta(y^i|x)$.

It is possible to train VAE with the NEO algorithm using the unbiased estimate of the normalizing constant to construct an ELBO. This approach is described in the supplement Appendix E. It is assumed here that the VAE has been trained and we are only interested in the sampling problem. In our experiment, we use a VAE trained on CelebA dataset [2] [16]. We consider the Block Gibbs inpainting task introduced in [15, Section 5.2.2]. We in-paint the bottom of an image using Block Gibbs sampling. Given an image y, denote by $[y^t, y^b]$ the top and the bottom half pixels. A two-stage Gibbs sampler amounts to (a) sampling $p_{\theta^*}(x|y^t, y^b)$ and (b) sampling $p_{\theta^*}(y^b|x, y^t) = p_{\theta^*}(y^b|x)$ (since y^b and y^t are independent conditional on x). Starting from an image y_0, we sample at each step $x_k \sim p_{\theta^*}(y \mid y_k)$ and then $\tilde{y}_k \sim p_{\theta^*}(y \mid x_k)$. We then set $y_{k+1} = (y_*^t, \tilde{y}_{k+1}^b)$. Stage (b) is elementary but stage (a) is challenging. We use the following decomposition of $p_{\theta^*}(x \mid y) = q_{\phi^*}^{\beta}(x \mid y) p_{\theta^*}(x, y) / (q_{\phi^*}^{\beta}(x \mid y) p_{\theta^*}(y))$ with $\beta \in (0, 1)$. We identify the *proposal* $\rho(x) \propto q_{\phi^*}^{\beta}(x \mid y)$, the *likelihood* $\mathrm{L} \leftarrow p_{\theta^*}(x, y)/q_{\phi^*}^{\beta}(x \mid y)$ and the normalizing constant $\mathrm{Z} = p_{\theta^*}(y)$ and apply i-SIR and NEO-MCMC sampler for stage (a). We compare different algorithms in stage (a): i-SIR, HMC and NEO-MCMC, with the same computational complexity ($N = 10$, $K = 12$, $\gamma = 0.2$ for NEO-MCMC, $N = 120$ for i-SIR, and HMC is run with $K = 20$ leap-frog steps). For each algorithm, 10 steps are performed. Figure 4 displays the evolution of the resulting Markov chains. The samples clearly illustrate that NEO-MCMC mixes better than i-SIR and HMC. More are showcased in the supplementary.

6 Conclusion

In this paper, we have proposed a new family of algorithms, NEO, for computing normalizing constants and sampling from complex distributions. This methodology comes with asymptotic and non-asymptotic convergence guarantees. For normalizing constant estimation, NEO-IS compares favorably to state-of-the-art algorithms on difficult benchmarks. NEO-MCMC is also very efficient for sampling complex distributions: it is particularly well-adapted to sampling multimodal distributions, thanks to its proposal mechanism which avoids being trapped in local modes. There are numerous potential extensions to this work. For example, it would be interesting to consider deterministic transformations other than conformal Hamiltonian dynamics integrators. These transformations could be trained, as for Neural IS, using a variation lower bound. It would also be interesting to further investigate the influence of the mixture weights $\{\varpi_k\}_{k \in \mathbb{Z}}$ on the efficiency of NEO.

Broader impact: Sampling from complex target distributions and computing their normalizing constants has numerous applications. Our work proposes novel methods to address such problems and has thus potential applications in many areas. This work does not present any foreseeable societal consequence.

[2] See https://github.com/YannDubs/disentangling-vae/tree/master/results/betaH_celeba

Bibliography

[1] Agapiou, S., Papaspiliopoulos, O., Sanz-Alonso, D., and Stuart, A. Importance sampling: Intrinsic dimension and computational cost. *Statistical Science*, pp. 405–431, 2017.

[2] Akyildiz, Ö. D. and Míguez, J. Convergence rates for optimised adaptive importance samplers. *Statistics and Computing*, 31(2):1–17, 2021.

[3] Andrieu, C., Doucet, A., and Holenstein, R. Particle Markov chain Monte Carlo methods. *Journal of the Royal Statistical Society: Series B (Statistical Methodology)*, 72(3):269–342, 2010.

[4] Bingham, E., Chen, J. P., Jankowiak, M., Obermeyer, F., Pradhan, N., Karaletsos, T., Singh, R., Szerlip, P., Horsfall, P., and Goodman, N. D. Pyro: Deep universal probabilistic programming. *The Journal of Machine Learning Research*, 20(1):973–978, 2019.

[5] Burda, Y., Grosse, R., and Salakhutdinov, R. Importance weighted autoencoders. In *The 4th International Conference on Learning Representations (ICLR)*, 2016.

[6] Che, T., Zhang, R., Sohl-Dickstein, J., Larochelle, H., Paull, L., Cao, Y., and Bengio, Y. Your GAN is secretly an energy-based model and you should use discriminator driven latent sampling. *arXiv preprint arXiv:2003.06060*, 2020.

[7] Chopin, N. and Robert, C. P. Properties of nested sampling. *Biometrika*, 97(3):741–755, 2010.

[8] Craiu, R. V. and Lemieux, C. Acceleration of the multiple-try metropolis algorithm using antithetic and stratified sampling. *Statistics and computing*, 17(2):109, 2007.

[9] Del Moral, P., Doucet, A., and Jasra, A. Sequential Monte Carlo samplers. *Journal of the Royal Statistical Society: Series B*, 68(3):411–436, 2006.

[10] Ding, X. and Freedman, D. J. Learning deep generative models with annealed importance sampling. *arXiv preprint arXiv:1906.04904*, 2019.

[11] El Moselhy, T. A. and Marzouk, Y. M. Bayesian inference with optimal maps. *Journal of Computational Physics*, 231(23):7815–7850, 2012.

[12] Franca, G., Sulam, J., Robinson, D. P., and Vidal, R. Conformal symplectic and relativistic optimization. *arXiv preprint arXiv:1903.04100*, 2019.

[13] Jia, H. and Seljak, U. Normalizing constant estimation with Gaussianized bridge sampling. In *Symposium on Advances in Approximate Bayesian Inference*, pp. 1–14. PMLR, 2020.

[14] Kingma, D. P. and Welling, M. Auto-encoding variational Bayes. *arXiv preprint arXiv:1312.6114*, 2013.

[15] Levy, D., Hoffman, M. D., and Sohl-Dickstein, J. Generalizing Hamiltonian Monte Carlo with neural networks. In *6th International Conference on Learning Representations, ICLR 2018, Vancouver, BC, Canada, April 30 - May 3, 2018, Conference Track Proceedings*. OpenReview.net, 2018. URL https://openreview.net/forum?id=B1n8LexRZ.

[16] Liu, Z., Luo, P., Wang, X., and Tang, X. Large-scale celebfaces attributes (celeba) dataset. *Retrieved August*, 15(2018):11, 2018.

[17] Maddison, C. J., Paulin, D., Teh, Y. W., O'Donoghue, B., and Doucet, A. Hamiltonian descent methods. *arXiv preprint arXiv:1809.05042*, 2018.

[18] Müller, T., McWilliams, B., Rousselle, F., Gross, M., and Novák, J. Neural importance sampling. *ACM Transactions on Graphics*, 38(145), 2019.

[19] Neal, R. M. Annealed importance sampling. *Statistics and Computing*, 11:125–139, 2001.

[20] Owen, A. and Zhou, Y. Safe and effective importance sampling. *Journal of the American Statistical Association*, 95(449):135–143, 2000.

[21] Papamakarios, G., Nalisnick, E., Rezende, D. J., Mohamed, S., and Lakshminarayanan, B. Normalizing flows for probabilistic modeling and inference. *arXiv preprint arXiv:1912.02762*, 2019.

[22] Prangle, D. Distilling importance sampling. *arXiv preprint arXiv:1910.03632*, 2019.

[23] Rotskoff, G. and Vanden-Eijnden, E. Dynamical computation of the density of states and Bayes factors using nonequilibrium importance sampling. *Physical Review Letters*, 122(15):150602, 2019.

[24] Rubin, D. B. Comment: A noniterative sampling/importance resampling alternative to the data augmentation algorithm for creating a few imputations when fractions of missing information are modest: The SIR algorithm. *Journal of the American Statistical Association*, 82(398): 542–543, 1987.

[25] Ruiz, F. J., Titsias, M. K., Cemgil, T., and Doucet, A. Unbiased gradient estimation for variational auto-encoders using coupled Markov chains. *arXiv preprint arXiv:2010.01845*, 2020.

[26] Shestopaloff, A. Y., Neal, R. M., et al. Sampling latent states for high-dimensional non-linear state space models with the embedded hmm method. *Bayesian Analysis*, 13(3):797–822, 2018.

[27] Skare, Ø., Bølviken, E., and Holden, L. Improved sampling-importance resampling and reduced bias importance sampling. *Scandinavian Journal of Statistics*, 30(4):719–737, 2003.

[28] Skilling, J. Nested sampling for general Bayesian computation. *Bayesian Analysis*, 1(4): 833–859, 2006.

[29] So, M. K. Bayesian analysis of nonlinear and non-gaussian state space models via multiple-try sampling methods. *Statistics and Computing*, 16(2):125–141, 2006.

[30] Tokdar, S. T. and Kass, R. E. Importance sampling: a review. *Wiley Interdisciplinary Reviews: Computational Statistics*, 2(1):54–60, 2010.

[31] Turner, R., Hung, J., Frank, E., Saatchi, Y., and Yosinski, J. Metropolis-Hastings generative adversarial networks. In *International Conference on Machine Learning*, pp. 6345–6353. PMLR, 2019.

[32] Wirnsberger, P., Ballard, A. J., Papamakarios, G., Abercrombie, S., Racanière, S., Pritzel, A., Rezende, D. J., and Blundell, C. Targeted free energy estimation via learned mappings. *arXiv preprint arXiv:2002.04913*, 2020.

[33] Wu, Y., Burda, Y., Salakhutdinov, R., and Grosse, R. On the quantitative analysis of decoder-based generative models. *arXiv preprint arXiv:1611.04273*, 2016.

Checklist

1. For all authors...
   (a) Do the main claims made in the abstract and introduction accurately reflect the paper's contributions and scope? [Yes]
   (b) Did you describe the limitations of your work? [Yes] See Section 6
   (c) Did you discuss any potential negative societal impacts of your work? [No] Our work is of theoretical and methodological nature.
   (d) Have you read the ethics review guidelines and ensured that your paper conforms to them? [Yes]
2. If you are including theoretical results...
   (a) Did you state the full set of assumptions of all theoretical results? [Yes] Assumptions are discussed in the theorem statements
   (b) Did you include complete proofs of all theoretical results? [Yes] The proof not included in main paper are in supplementary

3. If you ran experiments...
   (a) Did you include the code, data, and instructions needed to reproduce the main experimental results (either in the supplemental material or as a URL)? [Yes]
   (b) Did you specify all the training details (e.g., data splits, hyperparameters, how they were chosen)? [Yes]
   (c) Did you report error bars (e.g., with respect to the random seed after running experiments multiple times)? [Yes]
   (d) Did you include the total amount of compute and the type of resources used (e.g., type of GPUs, internal cluster, or cloud provider)? [Yes] See discussion in supplementary.
4. If you are using existing assets (e.g., code, data, models) or curating/releasing new assets...
   (a) If your work uses existing assets, did you cite the creators? [Yes]
   (b) Did you mention the license of the assets? [Yes]
   (c) Did you include any new assets either in the supplemental material or as a URL? [Yes]
   (d) Did you discuss whether and how consent was obtained from people whose data you're using/curating? [N/A]
   (e) Did you discuss whether the data you are using/curating contains personally identifiable information or offensive content? [N/A]
5. If you used crowdsourcing or conducted research with human subjects...
   (a) Did you include the full text of instructions given to participants and screenshots, if applicable? [N/A]
   (b) Did you describe any potential participant risks, with links to Institutional Review Board (IRB) approvals, if applicable? [N/A]
   (c) Did you include the estimated hourly wage paid to participants and the total amount spent on participant compensation? [N/A]